International Journal of Geophysics and Geochemistry
2015; 2(3): 29-38
Published online April 30, 2015 (http://www.aascit.org/journal/ijgg)

AASCIT American Association for Science and Technology


**Keywords**
Natural Gamma Ray Logs,
Radioelement Abundances,
Namorado Oil Field,
Turbidity Channels,
Campos Basin,
Brazil

Received: March 30, 2015
Revised: April 13, 2015
Accepted: April 14, 2015

# Distribution of Uranium, Thorium and Potassium in the Upper Macaé Formation, Campos Basin, Brazil: Estimates Based on Natural Gamma Ray Logs

**Eara de Souza Luz Oliveira, Valiya M. Hamza***

Observatório Nacional, Rio de Janeiro, Brazil

## Email address
hamza@on.br (V. M. Hamza)

## Citation
Eara de Souza Luz Oliveira,Valiya M. Hamza. Distribution of Uranium, Thorium and Potassium in the Upper Macaé Formation, Campos Basin, Brazil: Estimates Based on Natural Gamma Ray Logs. *International Journal of Geophysics and Geochemistry.* Vol. 2, No. 3, 2015, pp. 29-38.

## Abstract
Results of natural gamma logs in 39 deep wells have been used for estimating distributions of radioelements (Uranium, Thorium and Potassium) in the Namorado oil field of the Campos basin, in the southeastern continental margin of Brazil. The methodology adopted makes use of an optimization program based on simplex algorithm in inverting results of gamma and density logs for determinations of radioelements and radiogenic heat production. Successful application of the method has been verified using both synthetic and real data. Test runs with synthetic data are found to provide results within 95% confidence level. Tests with real indicated agreement within the limits of experimental uncertainty. Analysis of results for Namorado oil field have allowed identification of characteristic features in the vertical and lateral distributions of radioactive elements. Most of the sand and shale sequences in this oil field area are characterized by relatively low concentrations of uranium, generally in the range of 0.5 to 5ppm. On the other hand, concentrations of thorium are found to be relatively high, with values generally in the range of 2 to 10 pm. Potassium abundances are found to fall in the normal range of 1 to 8%. Maps of the spatial distributions of radioelement abundances and radiogenic heat indicate the presence of sinuous belts that are nearly coincident with the trajectories of turbidity currents inferred in geologic studies. It is proposed that the method of the present work may be used to map migration trends of radionuclides during subsidence history of continental margins.

## 1. Introduction

Measurements of natural gamma radiations are usually carried out as part of standard geophysical well logs in petroleum exploration wells. It is customary practice to express the results of such logs, designated usually as GR logs, in API units, which is an integrated measure of gamma radiations emitted by the naturally radioactive elements, present in the geologic medium adjacent to the well bore [1]. Usually, the radiation detectors employed in natural gamma logs are of low energy resolution and are incapable of providing information on the abundances of natural radioelements (uranium, thorium and potassium) that contribute to the overall sensor response. Consequently, availability of well logs providing abundances of radioelements (U, Th and K) are considerably limited. This problem has led to major difficulties in understanding the specific patterns of migration and transport of individual radionuclides in sedimentary environments.

In many cases however, such difficulties can be overcome by employing methods based on the SIMPLEX algorithm, widely used in linear programing[2]. For example, the proposed approach has the advantage that it can easily be adapted for extracting information on abundances of natural radioelements (U, Th and K) from results of natural gamma ray (GR) logs of deep oil wells. In the present work, we report results obtained in determining relative abundances of radioelements from data on natural gamma ray (GR) logs of oil wells in the Namorado petroleum field in the Campos basin, situated in the southeast continental margin of Brazil.

## 2. Study Area

The Campos Basin is the most prolific oil-producing basin in the western South Atlantic, with more than sixty hydrocarbon accumulations, currently accounting for about 80% of Brazilian oil production. The main oil accumulations occur in the Namorado sandstone of lower Cenomanian age, which composes the sedimentary sequences in the upper parts of Macaé formation. Analysis of core samples recovered in exploratory drilling have allowed identification of depositional sequences [3, 4, 5]The main reservoir is actually a succession of sandstones interbedded with layers of marga, shale, silt and calclutites with bioturbation.

The locations of the main oil fields of the Campos basin are indicated as yellow colored patches in the map of Fig. 1.Note that most of the oil fields are situated along a NE – SW trending belt, between the shallow and deep-water sections of the Campos basin. The present work has been carried out using data acquired in wells drilled in the Namorado oil field, the location of which is indicated by the black square in this figure. Results of exploratory drilling and detailed seismic surveys have allowed identification of the limits of the Namorado oil field. These are indicated as white colored narrow belts  in Fig. 2. Also indicated in this figure are the five major internal blocks of this oil field, as well as areas of accumulations of oil (patches of dark green), gas (patches of yellow) and water (patches of light green). The locations of exploratory wells, referred to in the present work are indicated as white dots.

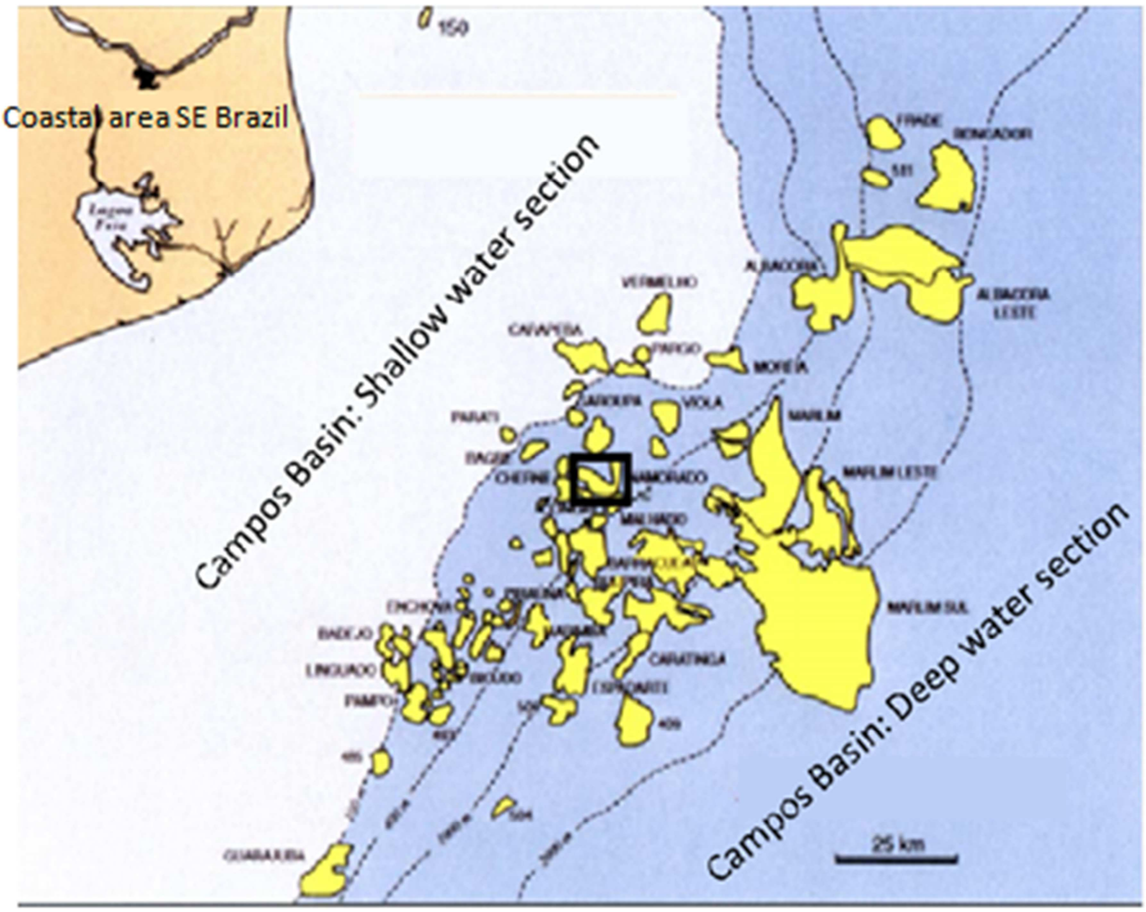


*Fig. 1. Location map of the Campos basin, in the continental margin of southeast Brazil. The yellow colored patches indicate the main oil fields. The black square indicate the location of the Namorado oil field, referred to in the present work.*

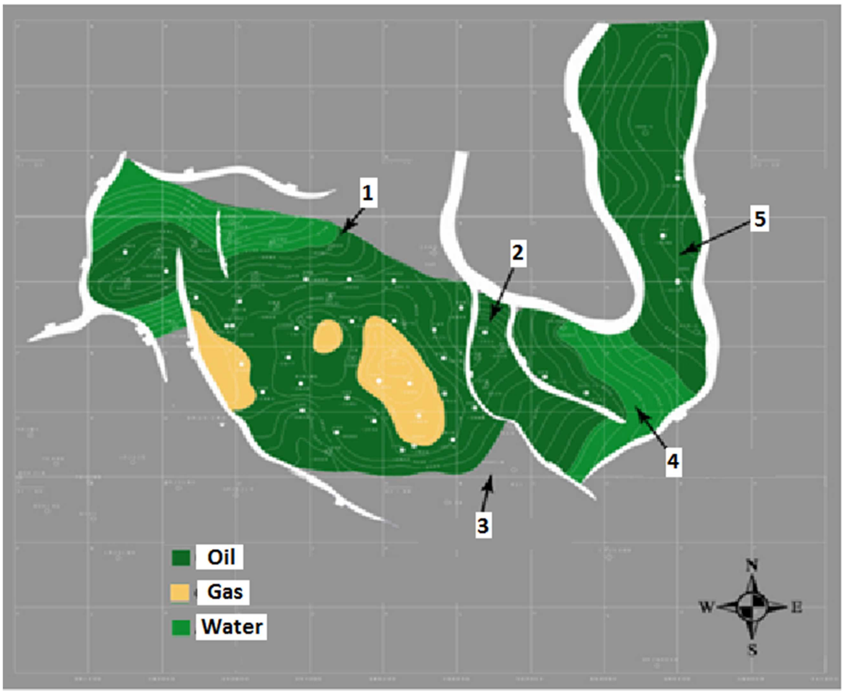


*Fig. 2. Map of the Namorado oil field in the Campos basin, indicating internal blocks that host accumulations of oil, gas and water. The white dots indicates locations of exploratory wells referred to in the present work (Adapted from [6]).*

Seismic surveys [7] coupled with analysis of stratigraphic sequences have allowed development of depositional models that outline the turbidity deposits in oil field areas of the Campos basin. A remarkable feature in the results of these models are the presence of channel like features extending from the continental margin to the deep-water sectors of the basin. According to the evolutionary model proposed by [8], turbidity currents had its beginning in the early periods of deposition but the channels associated with currents were covered sediment depositions during later periods. An example of the evolutionary sequences considered in such model sis reproduced in Fig. 3.

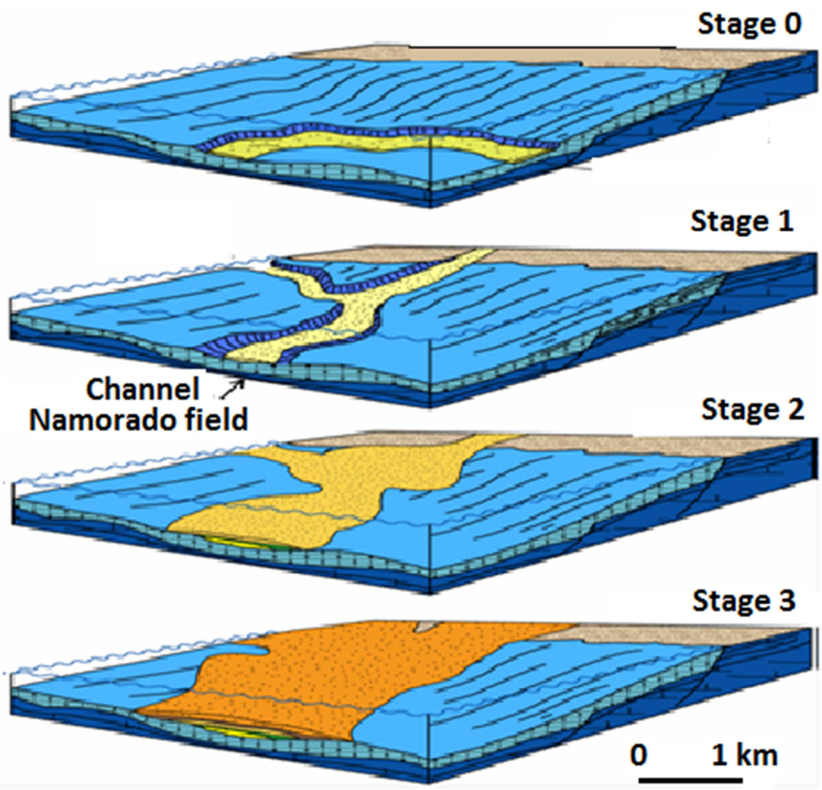


***Fig. 3.*** *Model of evolutionary sequences of Turbidite in the Campos basin (adapted from [8]).*

# 3. Methodology

In the present work, use has been made of a procedure based on the simplex algorithm in determining relative abundances of radioelements from results of natural gamma logs of oil wells in the Namorado petroleum field. The simplex is a popular method for solving problems in linear programming. It tests adjacent vertices of the feasible set (which is a polytope) in sequence so that at each new vertex the objective function improves or is unchanged. The shape of this polyporeis defined by the constraints applied to the objective function. If the objective function has a minimum value on the feasible region then it has this value on (at least) one of the extreme points [9]. This in itself reduces the problem to a finite computation since there is a finite number of extreme points. There is a straightforward process to convert any linear program into one in standard form so this results in no loss of generality.

The standard formulation of linear programing problem is minimization of a linear objective function subject to linear inequality constraints. In vector and matrix notation, we may write:

$$\min z = cx \tag{1}$$

subject to the condition that

$$Ax \leq b \tag{2}$$

where$z$ is the linear objective function to be minimized, $x = [x_1, \ldots, x_n]^{\perp}$ is a column-vector of $n$ non-negative decision variables, $c = [c_1, \ldots, c_n]$is a row-vector of coefficients, $A$ an n×m matrix of constraints, and $b = [b_1, \ldots, b_m]^{\perp}$a column vector of coefficients. The constraints may be two sided $b_{min} \leq Ax \leq b_{max}$ or with lower and upper bounds $x_{min} \leq x \leq x_{max}$. In the case of models with two decision variables, each linear inequality constraint divides the plane into feasible and infeasible regions. The first one is a convex polygon formed as the intersection of these regions. The objective function is a direction in the plane. The optimum solution is always in some corner of this polygon.

The computational procedure adopted in the present work makes use of the function "LINPROG" in MATLAB [10]. The objective function adopted for this purpose is the relation for radiogenic heat (A):

$$A\,[\mu W/m^3] = 10^{-5}\rho(9.52\,C_U + 2.56\,C_{Th} + 3.48\,C_K) \tag{3}$$

In the above equation (proposed initially by [11, 12]), $C_u$ and $C_{th}$ are respectively the abundances of uranium and thorium in ppm, $C_k$ is abundance of potassium in percent and ρ is density in kg/m$^3$. The constraints applied to the objective function are based on the relation between intensity of radiation in gamma ray logs (GR) and concentrations of radionuclides as described in equation (3):

$$GR_{obs} = 10^{-3}\rho(6.57C_U + 1.77C_{Th} + 2.40C_K) + 5.0 \tag{4a}$$

$$GR_{obs} \geq 0^{-3}\rho(6.03C_U + 1.62C_{Th} + 2.20C_K) + 0.8 \tag{4b}$$

In addition, it was found necessary to adopt suitably selected values for the concentrations of radionuclides in limiting the process of optimization. In the present case, the following values selected, based on data reported by [13] and [14]:

$$0.0 \leq C_U \leq 6.0\text{ppm}, \quad 0.0 \leq C_{Th} \leq 20.0\text{ppm}, 0.0 \leq C_K \leq 15\% \tag{5}$$

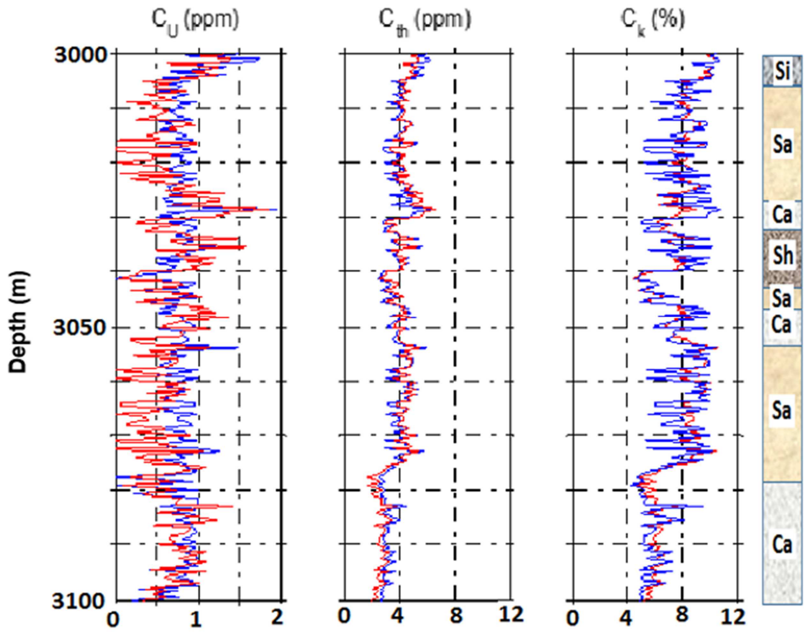


***Fig. 4.*** *Results of tests with synthetic data for a hypothetical well. Red curves indicate synthetic data before optimization while blue curves represent results obtained after the optimization. The column on the right indicates the lithology (Si – Silt; Sa – sandstone; Ca – Calclutite; Sh – Shale)*

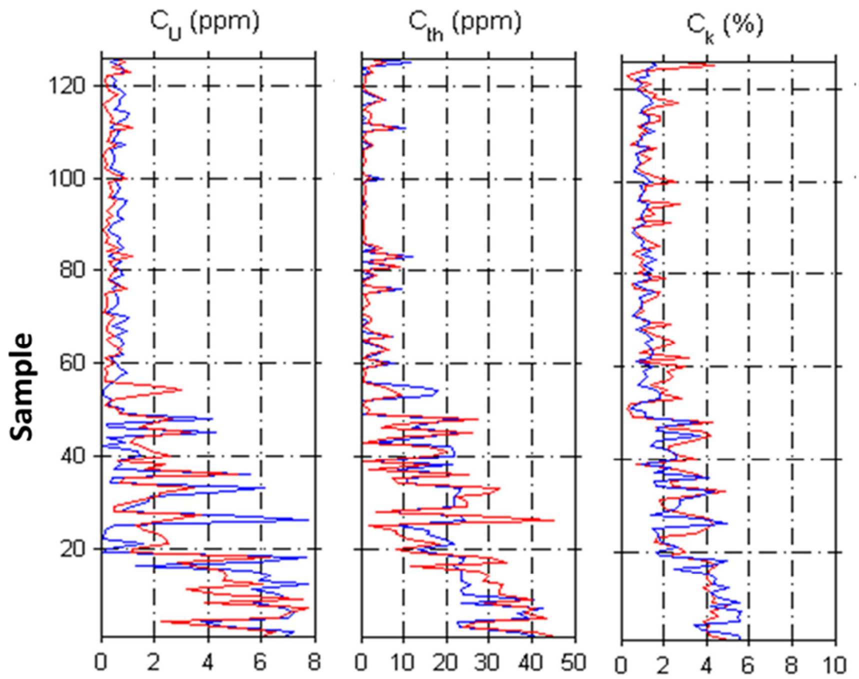


***Fig. 5.*** *Results of tests with data reported in works of Reyes (2008) and Sapucaia et al (2005). Red curves indicate synthetic data before optimization while blue curves represent results obtained after the optimization.*

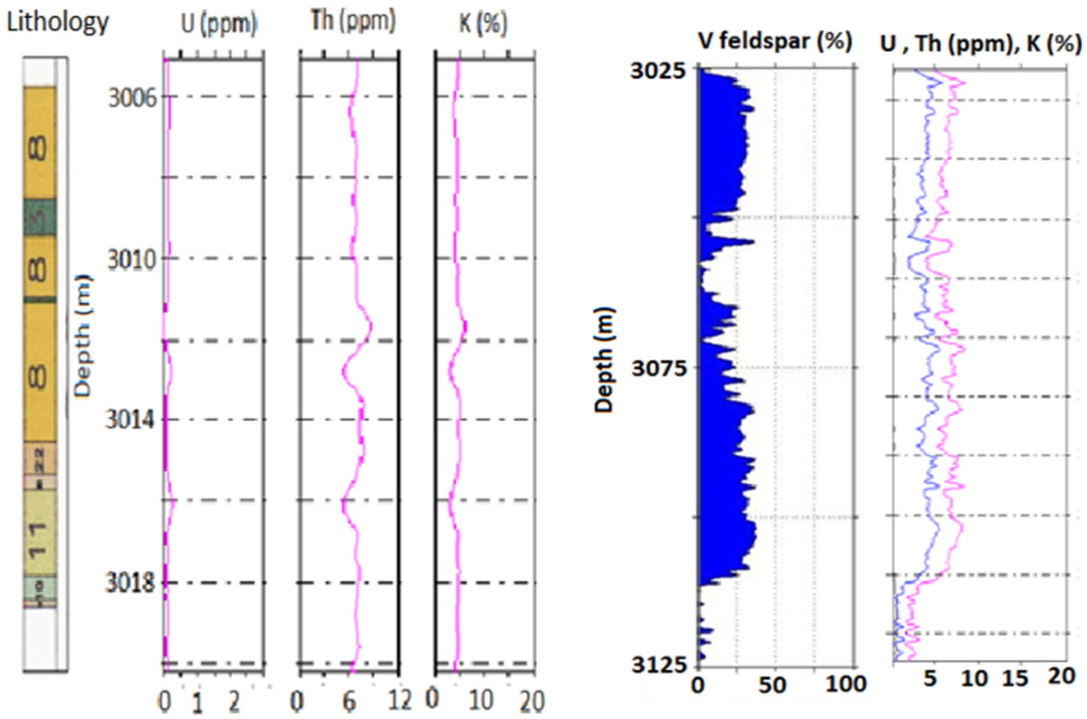


***Fig. 6.*** *Vertical variations of radioelementsin well Na-01. The left panel indicate variations associate with litho logy. The numbers in the left column of this panel indicates the litho types identified in core analysis (6 – Coarse grained sandstone; 8- Medium grained sandstone; 9- Cemented sandstone; 10- Intercalated sequence of shale and sandstone). The right panel indicates variations of radioelements associated with changes in volume of feldspar.*

The operational aspects of the computational procedure were verified using test runs employing both synthetic and real data[15].The results of tests with synthetic data for a hypothetic well cutting across six different rock types is presented in Fig. 4. The results of tests with data reported in the works of [16] and [17] are presented in Fig. 5. In both figures, the red curves indicate synthetic data before optimization and the blue curves represent results obtained after the optimization. It is clear that the computational scheme employed in optimization process has been remarkably successful in reproducing the abundance values within the limits of experimental errors.

## 4. Comparison with Results of Core Analysis

Comparison with results of core analysis of deep wells is another convenient means of evaluating the relative merits of the methodology described in the previous section. A careful examination of the data set provided by the National Agency for Petroleum (ANP) allowed selection of four wells (Na01, Na04, Na07 and Na11) for which results of core analysis and natural gamma ray logs were available. According to results of core analysis, the lithological sequences encountered in well Na01 are mainly sandstones, diamectites and layers with intercalated sequences of shale and sandstone. The nature of vertical variations of radioactive elements associated with changes in lithological sequences of well Na01 is illustrated in the left panel of Fig. 6. Eleven litho-facies (five in the interval of 2971 to 2990m and six in the interval 3005 to 3021 m) have been identified in well Na01. Results of core analysis have also allowed determination of feldspar minerals [18].The right panel of Fig. 6 illustrates the variations in volume of feldspar and its remarkable correlation with the distribution of radioelements.

## 5. Gamma Ray (GR) Logs and Radiogenic Heat Production

Comparison of the results of natural gamma ray logs with vertical distributions of radionuclides derived using the SIMPLEX method have been attempted for four wells in the Namorado oil field. The results for well Na01 are presented in Fig. 7, where the left column indicate the record of gamma ray log and the middle column the vertical variations of U, Th and K. The red and black colored curves in the middle column indicate distributions of thorium and uranium (abundances in ppm) respectively. The potassium abundances (in %) are indicated by the blue curve. Note that the uranium abundances (in ppm) are extremely low compared to those of thorium.

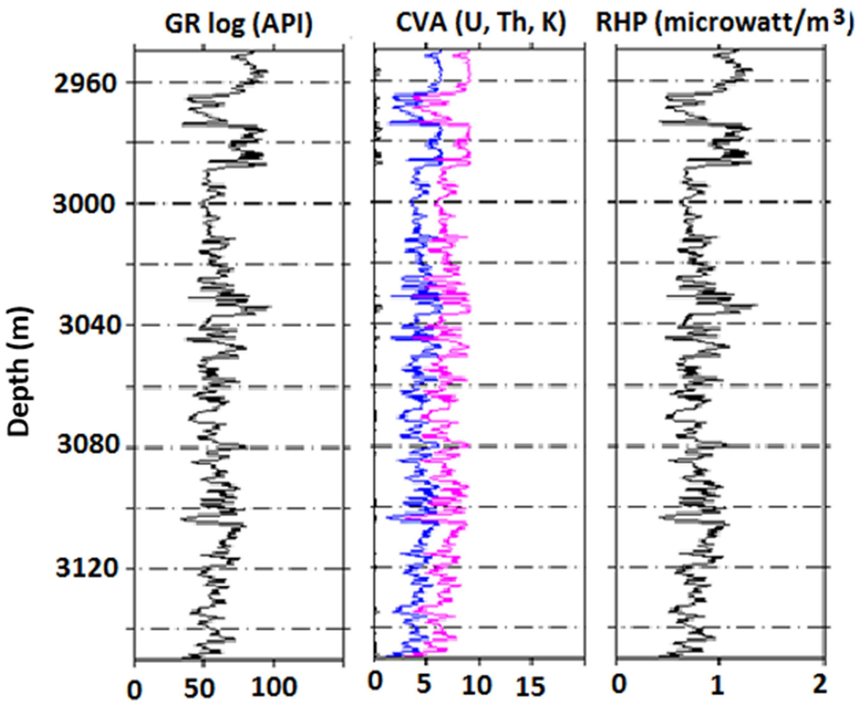


***Fig. 7.*** *Comparison of natural gamma ray log and vertical distributions of radioelement abundances (U, Th and K) and radiogenic heat production in well Na01.*

The vertical distributions of radionuclides are presented in Fig.8 for wells Na-04 and Na-07. As in the case of Fig.7 the red and black colored curves in the middle panel indicate distributions of thorium and uranium (abundances in ppm) respectively. The uranium abundancesare extremely low compared to those of thorium. The distribution of potassium follows trends that are similar to those of thorium. The litho logical sequences encountered in these wells include mainly sandstones, siltstones, shale and marga,diamectites and layers with intercalated sequences of shale and sandstone.

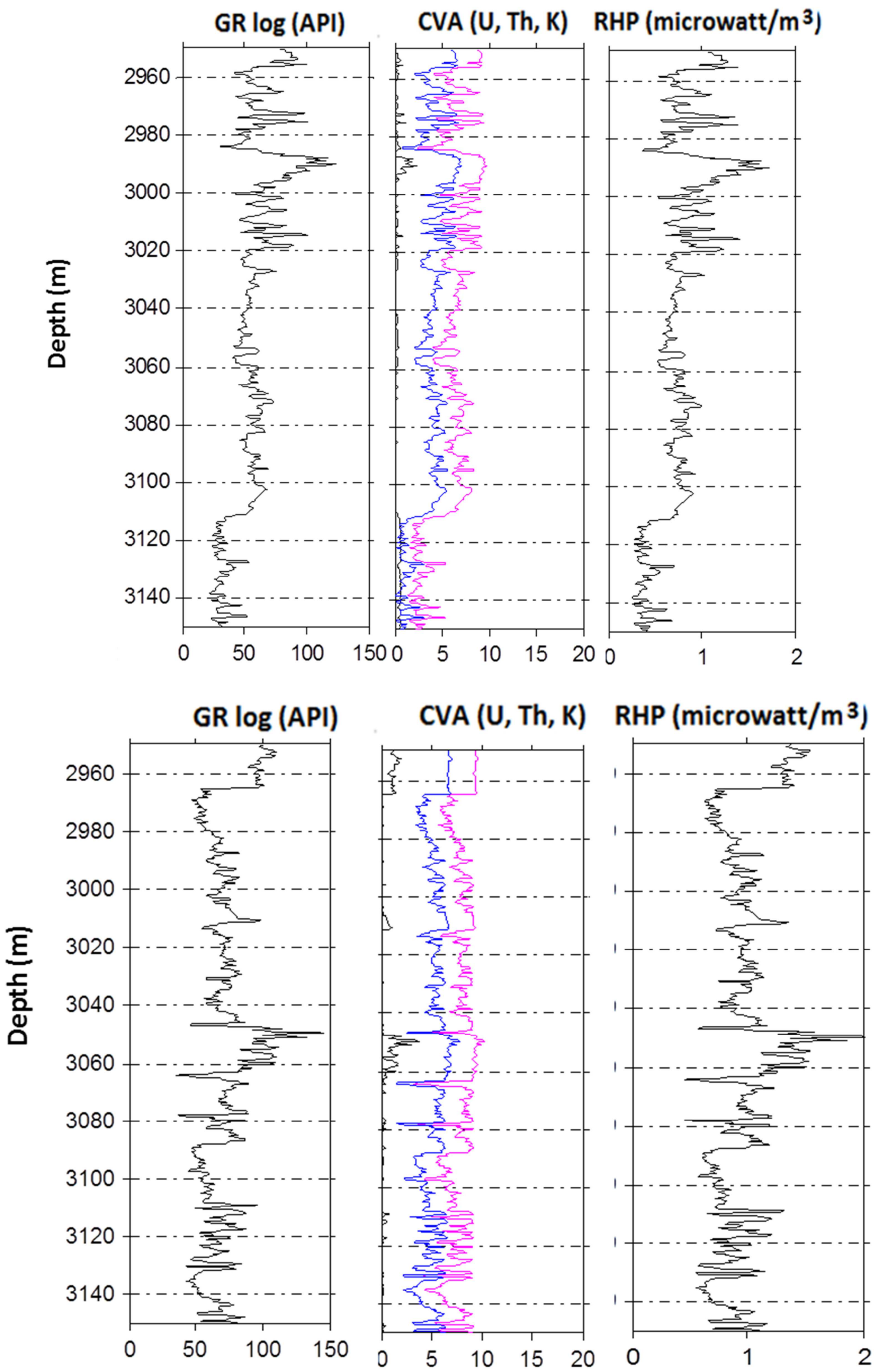


***Fig. 8.*** *Comparison of natural gamma ray logs and vertical distributions of radioelement abundances (U, Th and K) and radiogenic heat production (RHP) in wells Na-04 (upper panel) and well Na-07 (down panel).*

## 6. Lateral Variations of Radio Elements in the Namorado Oil Field

The availability of results of the optimization process based on natural gamma ray logs provides an opportunity to examine spatial distributions of radioelement abundances. In the present work, results of natural gamma ray logs for 39 wells were employed for determining spatial distributions of radioelement abundances in the Namorado oil field.

The map of Fig.9 illustrates the distribution of uranium at the depth level of 3100 meters. Note that the range of values are in the interval of 0 to 5 ppm. Most of the Namorado oil field is characterized by uranium values of less than 1 ppm. A remarkable feature in this figure is the presence of an approximate north – south trending narrow belt where values of uranium higher than 2 ppm occur. Note that the belt is wider at the northern sector compared to that in the southern sector. It is a consequence of relatively high values of uranium in wells situated along channels of turbidity flows, proposed by [8]. Distributions of thorium and potassium values, presented respectively in the maps of Figures 10 and 11, also reveal similar patterns.

The maps of Fig.10 illustrate the distributions of thorium and potassium at the depth level of 3100 meters. The thorium values are in the range of 4 to 10 ppm while potassium is in the range of 2 to 8%. The northern sectors of the oil field are characterized by relatively high values relative to those in the southern parts. Another notable feature is the presence of channel like feature identified in Fig. 9.

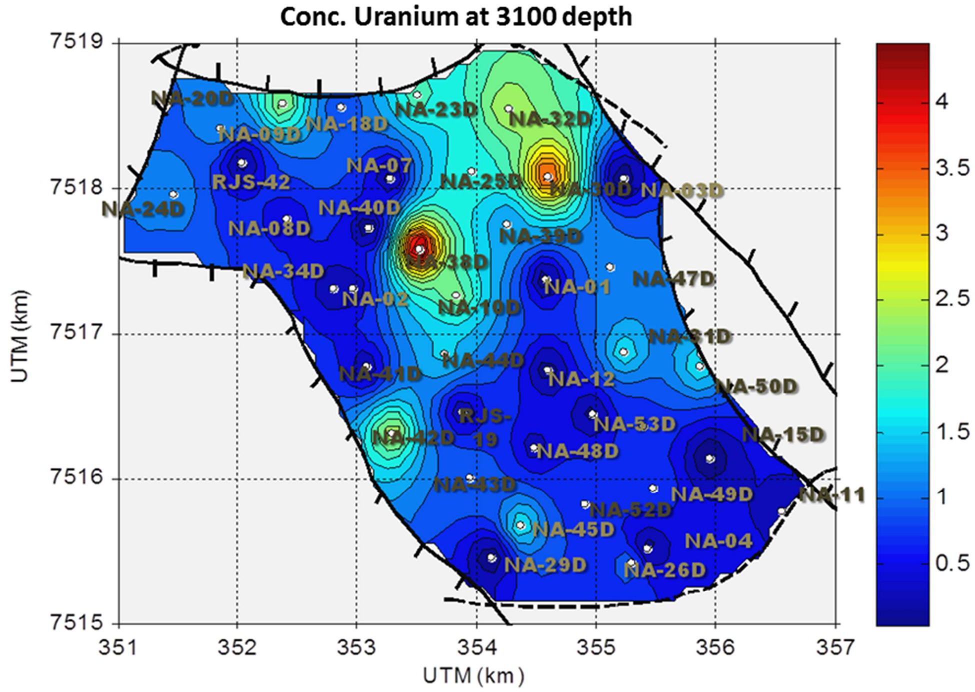


*Fig. 9. Map of the spatial distribution of uranium at the depth level of 3100m, in the main sector of the Namorado oil field, Campos basin.*

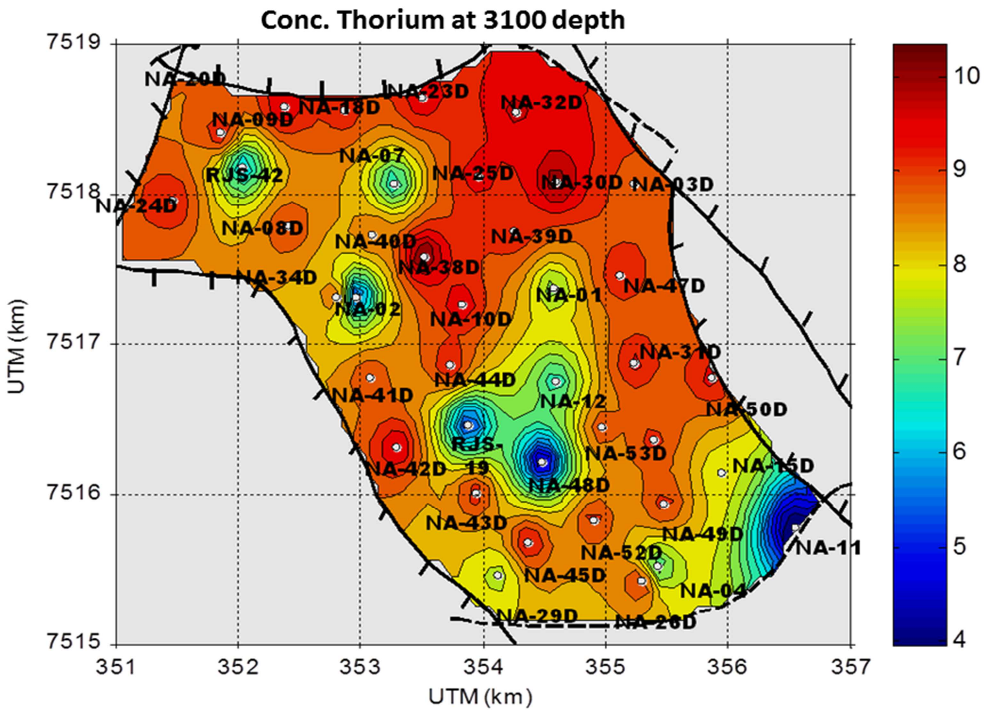

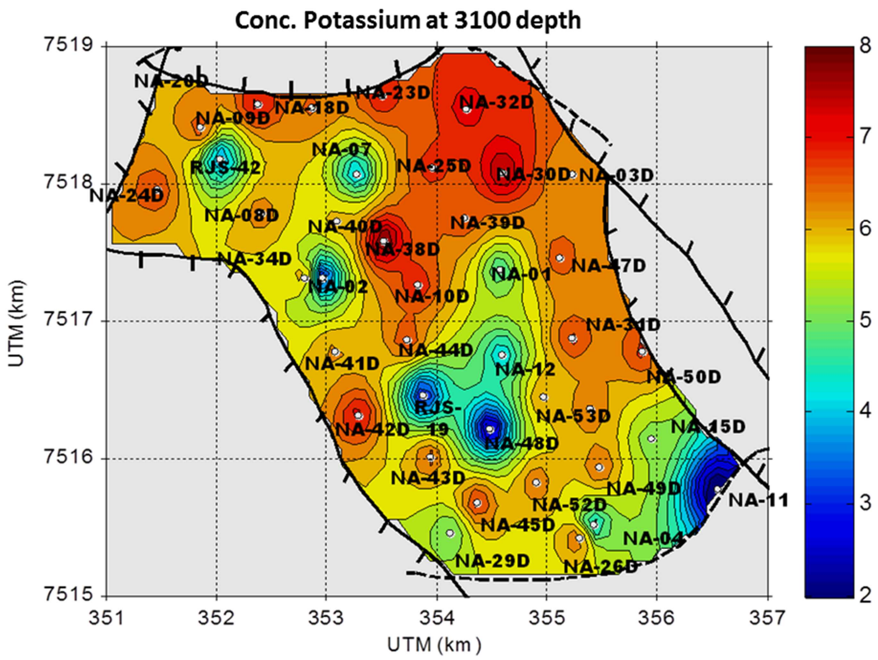


*Fig. 10. Maps of the spatial distribution of thorium (upper panel) and potassium (lower panel) at the depth level of 3100m, in the main sector of the Namorado oil field, Campos basin.*

A summary of the mean values of radioelement abundances is presented in Table 1, for the main rock types in the Namorado oil field. Interlaminated sequences of silt, shale and sandstone are found to have GR log values in excess of 80API units. Conglomerates and brecciaare found to have GR log values less than 50 API units. The remaining rock types have API values in the interval of 50 to 80.

*Table 1. Values of mean and standard deviations of natural gamma ray logs and abundances of U, Th and K.*

| Rock Type | GR (API) | U (ppm) | Th (ppm) | K (%) |
|---|---|---|---|---|
| Interlaminated silt and shale | 100.2 ± 1.8 | 2.5 ± 0.8 | 9.8 ± 0.2 | 7.3 ± 0.3 |
| Stratified silt and clay | 99.4 ± 0.6 | 1.1 ± 0.5 | 9.4 ± 0.2 | 6.7 ± 0.2 |
| Radioactive shale | 99.2 ± 5.5 | 0.7 ± 0.4 | 9.2 ± 0.2 | 6.5 ± 0.2 |
| Interlaminated sand, bioturbated | 89.3 ± 3.0 | 0.04 ± 0.01 | 7.9 ± 0.2 | 5.2 ± 0.2 |
| Shale and silt /Marga bioturbated | 73.5 ± 4.9 | 0.03 ± 0.03 | 8.3 ±0.5 | 5.6 ± 0.4 |
| Marga, bioturbated | 71.8 ± 1.9 | 0.03 ± 0.01 | 8.01± 0.3 | 5.3 ± 0.2 |
| Intercalated sandstone and shale | 58.4 ± 4.4 | 0.10 ± 0.04 | 6.8 ± 0.3 | 4.3 ± 0.5 |
| Interlaminated argillaceous silt | 55.2 ± 6.4 | 0.18 ± 0.07 | 5.8 ± 0.8 | 3.5 ± 0.6 |
| Medium grained Sandstone | 52.7 ± 2.8 | 0.14 ± 0.04 | 6.4± 0.4 | 3.9 ± 0.4 |
| Conglomerates, carbonated breccia | 29.6 ± 1.8 | 0.55 ± 0.03 | 2.3 ± 0.3 | 0.7 ± 0.2 |

## 7. Conclusions

According to results of the present work, most of the sand and shale sequences in Namorado oil field are characterized by relatively low concentrations of uranium. At 3100m depth, the concentrations of uranium values generally in the range of 0.5 to 5ppm. On the other hand, concentrations of thorium are found to be relatively high, with values generally in the range of 2 to 10 ppm. Potassium abundances are found to fall in the normal range of 1 to 8%. A summary of minimum, maximum and mean values of the radioelement abundances and heat generationare given in Table 2, for the depth level of 3100 m.

*Table 2. Values of mean and standard deviation of radioelement abundances ($C_u$, $C_{th}$ and $C_k$) along with respective values of upper and lower limits.*

| Description | $C_U$(ppm) | $C_{Th}$(ppm) | $C_K$(%) | Radiogenic Heat Production(μW/m$^3$) |
|---|---|---|---|---|
| Mean | 0.7 | 5.1 | 3.5 | 0.6 |
| Standard Deviation | 0.6 | 1.4 | 1.1 | 0.4 |
| Upper Limit | 4.2 | 9.5 | 7.4 | 1.3 |
| Lower Limit | 0.6 | 2.3 | 1.6 | 0.3 |

Maps of the spatial distributions of radioelement abundances and radiogenic heat production indicate the presence of sinuous belts that are nearly coincident with the trajectories of turbidity currents inferred in geologic studies. There are indications that these belts are characterized by relatively high values of uranium, thorium and potassium. It is proposed that the method of the present work may be used to map migration trends of radionuclides during subsidence history of continental margins.

## Acknowledgments

The database discussed in the present paper is part of public domain information for Namorado oil field, made available for academic research by the National Agency for Petroleum (ANP) of the federal government of Brazil.

Itwas carried out as part of Ph.D. thesis project of the first author. We thank Dr. Jorge Leonardo Martins (National Observatory – ON/MCTI, Rio de Janeiro) for his guidance and collaboration in the early phases of this thesis work.

We acknowledge the research scholarship granted to the first author for her thesis work by Cordenadoria de Aperfeiçoamen to Pesquisa e Ensino Superior - CAPES.

The second author is recipient of a research scholarship granted by ConselhoNacional de Desenvolvimento Cientifico e Tecnológico – CNPq (Project No. 301865/2008-6; Produtividade de Pesquisa - PQ).

## References

[1] Belknap, W.B., Dewan, J.T. Kirkpatricl, C.V., Mott, W.E., Pearson, A.J., and Rabson, W.R.(1959). “API calibration facility for nuclear logs: in Drilling and Production Practice”. *American Petroleum Institute, Houston*: pp. 289-317.

[2] Dantzig, G.B., Orden, A., Wolfe, P. (1955).“Generalized Method Simplex for Minimizing a Linear from Under Inequality restraints”. *Pacific Journal Math.*, 5: 183-95.

[3] [3} Borgui, L. (2000). “Visão Geral da Análise de Fácies Sedimentares do Ponto de Vista da Arquitetura Deposicional”. *Boletim do Museu Nacional, N.S., Geol., Rio de Janeiro*, 53: 1-26.

[4] Bacoccoli, G. Moraes, R.G. & Campos, O.A.J. (1980). “The Namorado Oil Field: A Major Oil Discovery in the Campos Basin, Brazil” In: *Giant Oil and Gas Fields of the Decade: 1968-1978. Tulsa: American Association of Petroleum Geologist Memoir*, 30: 329-38.

[5] Souza, Jr., O.G. (1997). “Stratigraphie Séquentielleet Modelisation Probabiliste des Reservoirs d’un Cône Sous-Marin Profond (Champ de Namorado, Brésil). Integration des Données Géologiqueset Géophisiques”. Ph. D. Thèse, Université Pierre et Marie Curie, 215 p.

[6] Menezes, S.X. (1990). “Modelo Hidrológico do Campo de Namorado”. Internal Report, PETROBRAS/DEPEX/DIRSUL.

[7] Augusto, F. O. A.(2009). “Mapas de Amplitude Sísmica para Incidência Normal no Reservatório Namorado, Bacia de Campos”. UnpublishedM.Sc. Thesis, Observatorio Nacional, Rio de Janeiro, RJ.

[8] Barboza, G.E.(2005). “Análise Estratigráfica do Campo de Namorado (Bacia de Campos) com base na Interpretação Sísmica Tridimensional”. Unpublished Ph.D. Thesis, UFRGS. RS.

[9] Murty, K.G. (1983)“Linear programming”, *John Wiley &Sons Inc., New York*: 482 pp

[10] MATLAB (200) “Version 8”. *The MathWorks Inc*., Natick, MA.

[11] Rybach, L. (1986) “Amount and significance of radioactive heat sources in sediments”: in *Thermal Modeling in Sedimentary Basins*, J.Burus (Ed) Editions Technip, Paris, 311 - 22.

[12] Bucker, C; Rybach, L. (1996). “A simple method to determine heat production from gamma-ray logs”. *Marine and Petroleum Geology,* 13(4):373-75.

[13] Wahl, L. S. (1983). “Gamma-ray logging”. *Geophysics*. 48:1536 – 50.

[14] Schlumberger, (2014).http://www.apps.slb.com/cmd/mineral.aspx, September 2015.

[15] Oliveira, E.S.L., Martins, J.L. (2011). “Modeling and Inversion of Gamma-Ray Logs: Estimation of Radionuclide Concentrations”. *Proceedings, 12th International Congress of the Brazilian Geophysical Society*, Rio de Janeiro, Brazil

[16] Reyes, L. M.G.(2008).“Distribuição vertical da taxa volumétrica de produção de calor radiogênico no Cráton do São Francisco”. *Unpublished Ph.D. Thesis, Institute of Geosciences, UFBA*, Salvador.

[17] Sapucaia, N.S., Argollo, R.M., Barbosa, J.S.F. (2005). “Teores de Potássio, Urânio, Tório e taxa de produção de calor radiogênico no embasamento adjacente às bacias sedimentares de Camamu e Almada, Bahia, Brasil”. *Rev. Bras. Geof.* 453-75.

[18] Magalhães, M. F., Martins, J.L. (2012). "Petrophysical Model for Bulk Density of Complex Lithologies" Brazilian Journal of Geophysics, 30(1): 63-79.